Biointerface Research in Applied Chemistry

Original Research Article

Open Access Journal

Correlation between composition and activity of gold nanoparticle conjugates with streptococcal protein G

Dmitriy V. Sotnikov [1], **Anatoly V. Zherdev [1]**, **Boris B. Dzantiev [1, *]**

[1]A.N. Bach Institute of Biochemistry, Federal Research Centre «Fundamentals of Biotechnology» of the Russian Academy of Sciences
Leninsky prospect 33, Moscow 119071, Russia

*corresponding author e-mail address: *boris.dzantiev@mail.ru* | Scopus ID 7006549067

ABSTRACT

The composition of the conjugates of gold nanoparticles with streptococcal protein G was studied using fluorescence spectroscopy. The method for determining the composition is based on measuring the intrinsic fluorescence of tryptophan as part of the protein. The equilibrium constants of protein binding by the gold surface were determined using the Sketchard method. An increase in the dissociation constant of the protein–nanoparticle complex for increasing the amount of bound protein was demonstrated, and a relationship was established between the stability of the conjugates, their antigen-binding activity, and the dissociation constant. The effectiveness of the conjugates of different compositions in immunochromatographic assay of specific antibodies against the lipopolysaccharide antigen of *Brucella abortus* was compared. The binding ability of the conjugates increased along with the amount of protein G to ~200 molecules per nanoparticle. A further increase in the amount of adsorbed protein led to a deterioration in the functional activity of the conjugates.

Keywords: *nanoparticle conjugate; streptococcal protein G; tryptophan; fluorescence; immunochromatographic assay.*

1. INTRODUCTION

Conjugates of gold nanoparticles (GNPs) with proteins are widely used in various fields of analytical chemistry and biochemistry [1-3]. In particular, GNP conjugates with immunoglobulin-binding proteins are commonly applied as detecting analytical reagents [4-7]. To choose the best protocol for adsorption immobilization of a protein on the GNP surface, the product of the adsorption process is typically controlled by flocculation (i.e., aggregation under high ionic strength) [8, 9]. Many authors recommend the use of conjugates with protein content slightly higher than the minimum concentration, preventing aggregation of GNPs in the presence of 10% NaCl [8-10]. It is assumed that this concentration provides covering the surface of GNPs and that its further increase is impractical.

However, there is evidence of sorption of proteins by GNPs at concentrations significantly higher than stabilizing ones. For example, Bell et al. showed a permanent growth in the hydrodynamic radius of GNP conjugates with proteins to the proteins' concentrations of 1 g/L or more, although the stabilizing concentrations determined by the flocculation method were 2 orders of magnitude lower [11]. It remains unclear why the increasing number of binding molecules on the particle does not always lead to the higher binding capacity of the conjugate [12].

These effects can be caused by several factors: a change in the orientation and conformation of adsorbed molecules, steric barriers to the interaction with tightly located molecules, partial desorption, or multilayer adsorption with obstruction of the lower layers [12].

In the past decade, the opinion has been established that the proteins on the surface of nanoparticles are subdivided on subpopulations of molecules that are bound through various mechanisms. Differences in binding constants for these subpopulations can reach several orders of magnitude. Such a structure of protein layers on the surface of nanoparticles is called the "hard and soft corona" [13-19]. Some authors associate hard corona with monolayer immobilization and soft corona with multilayer immobilization, noting that soft corona is easily desorbed from the surface, whereas hard corona practically does not dissociate [20, 21].

From a practical point of view, the information on the composition and stability of nanoparticle–protein conjugates is extremely important for obtaining them with maximal reactivity and effective consumption of reagents. At the moment, there is no information on the correlation of composition, the binding parameters of immobilized molecules, and the functional activity of the conjugates.

In the present study, the composition of GNP conjugates with streptococcal protein G was investigated using the previously developed technique based on fluorescence spectroscopy [22]. Streptococcal protein G was chosen for the study because of its wide immunoanalytical use [23-25]. The binding ability of the obtained conjugates in immunochromatographic assay (ICA), namely in the determination of specific antibodies against *Brucella abortus* lipopolysaccharide (LPS), was studied.

2. MATERIALS AND METHODS

Preparation of GNPs. First, 1 ml of a 1% hydrochloric acid (Sigma, USA) was mixed with 97.5 ml of water. The mixture was brought to a boil, and 2 ml of a 1% sodium citrate was added and stirred. The resulting mixture was boiled for 30 min, and then

cooled to room temperature (RT). The obtained preparation was stored at 4 °C. Dimensional parameters of the obtained GNPs were characterized by transmission electron microscopy (TEM) as earlier described at [26].

Determination of the GNP-stabilizing concentration of protein G. First, 1 ml of GNPs solution with $OD_{520} = 1.0$ was added to 0.1 ml of aqueous solution of protein G (preparation of 2018, Imtek, Russia) at concentrations from 1 to 13 µg/mL, and then mixed and incubated for 10 min at RT. Then, 0.1 ml of 10% NaCl was added to each sample and mixed. After 10 min, OD_{580} was measured, and a flocculation curve (the dependence of OD_{580} on protein concentration) was plotted. The stabilizing protein concentration, according to [27], was defined as the concentration corresponding to reaching the plateau of the flocculation curve plus 20%.

Characterization of protein G–GNPs conjugates. The amount of adsorbed protein G was determined according to [22]. The GNPs solution was poured into eight 2 ml tubes and centrifuged at 12,000 g, and the supernatant was taken. The GNP sediment was agitated (the volume of the remaining liquid in the tube was adjusted strictly to 0.2 ml with the supernatant). In the collected supernatant, protein G solutions were prepared at the following concentrations: 100, 50, 20, 10, 5, and 2 µg/ml, diluting the stock solution (100 mg/ml) by the supernatant. The resulting solutions were taken at 0.2 ml each and added to 0.2 ml of GNP solutions obtained after centrifugation. The remaining protein solutions were used for calibration. Protein and GNPs were incubated for 1 h and centrifuged at 12,000 g. Next, 0.2 ml of supernatant was collected and transferred to a microplate. Calibration solutions were also transferred, and fluorescence was measured. Fluorescence spectra were recorded on a Perkin Elmer En Spire 2300 microplate spectrophotometer (Waltham, MA, USA) in Nunc MaxiSorp white microplates at an excitation light wavelength of 280 nm in the emitted light wavelength range of 290–500 nm.

Preparation of immunochromatographic tests. The mdi Easypack membrane kit (Advanced Microdevices, India) comprising polyester-backed nitrocellulose membrane Type 90CNPH, conjugate release matrix PT-R5, whole blood separator Type FR1(0.6), and final absorbent pad AP045 was used. A GNP-protein G conjugate was applied (11 µL per centimeter of the strip) to a conjugate release matrix with the use of an IsoFlow dispenser (Imagene Technology, USA) at a dilution corresponding to $OD_{520} = 10$. The test zone was formed on a polyester-backed nitrocellulose membrane using *Br. abortus* LPS; 2 µL of the LPS solution (1.0 mg/mL in distilled water) was applied per centimeter of the strip. After the application of the reagents, the membranes were dried, assembled, cut, and hermetically packed as described earlier [27].

Immunochromatographic assay. The assay was carried out at room temperature. A test strip was vertically submerged into the sample for 1 min, removed, and placed horizontally. The results were recorded after 10 min from the assay beginning. The binding of the GNP was quantified using a portable digital video analyzer Reflekom (Russia).

3. RESULTS

Characterization of GNPs. The dimensional parameters of GNPs were evaluated using TEM. The preparation had an average diameter of 20.4 nm and a high degree of homogeneity; the average deviation did not exceed 3.5 nm in a sample of 112 particles.

Flocculation studies. The obtained dependence of OD_{580} on protein G concentration is shown in figure 1. Its appearance corresponds to the existing concept of protein conjugation with GNPs: OD_{580} first increases, reaches a maximum, and then decreases, reaching a plateau.
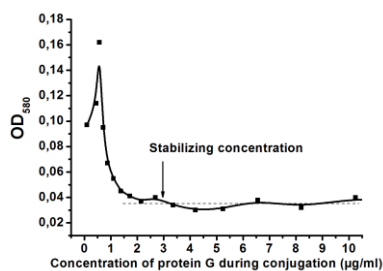

Figure 1. Flocculation curve for the GNPs covered by protein G. The X-axis shows the concentration of protein G, and the Y-axis shows the OD_{580} after adding 10% NaCl.

Testing conjugates in ICA. The antibody-binding capacity of the GNP conjugates with protein G of different compositions was comparatively tested in the immunochromatographic determination of antibodies against LPS of *Brucella abortus*. A cow serum—a national positive standard containing 1,000 IU of specific antibodies against the LPS—was used as the tested sample. The dependence of the color intensity of the test strip's analytical zone on the concentration of the protein G used for the conjugation is shown in figure 2.
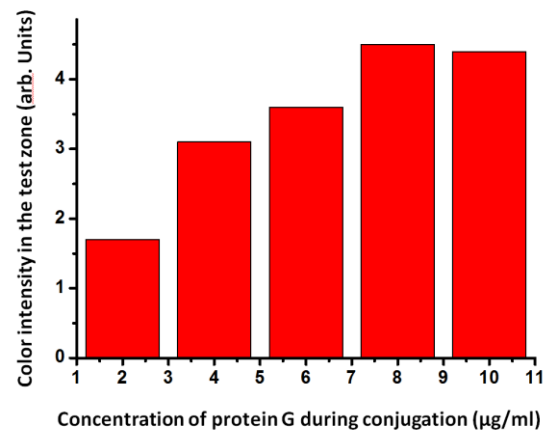

Figure 2. Label binding in ICA of standard positive serum using GNP conjugates with protein G of different compositions.

A comparison of the flocculation and ICA data leads to the conclusion that the activity of the conjugate is not directly dependent on the stabilization of the GNP surface by adsorbed protein molecules. The plateau of flocculation dependence was reached at 4 µg/mL, whereas the maximal binding in ICA was attained at 8 µg/ml. Thus, the affinity of the conjugate increased to a concentration that was double the threshold determined by particle stabilization. Two possible explanations for this phenomenon may be considered. First, the stabilization of nanoparticles with respect to the action of high ionic strength can be achieved before filling the monolayer. Second, an increase in the reactivity of conjugates can be related to the changing orientation of immobilized protein molecules.

Determination of the conjugates' composition. To establish the reasons for the change in the reactivity of the conjugates G, their composition was studied. To determine the amount of protein adsorbed on GNP, the protein's own fluorescence was used. Fluorescence was measured for protein solutions and for supernatants obtained after centrifugation of the conjugates (see fig. 3). The maximum emission was observed at 350 nm according to the known properties of the tryptophan [28].
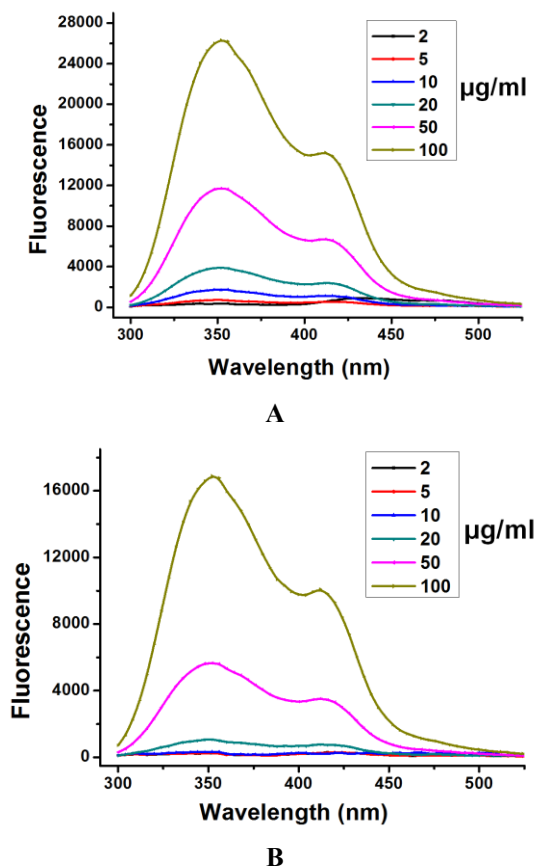

Figure 3. Fluorescence of protein G at an excitation wavelength of 280 nm. **A.** Spectra in the absence of GNPs. **B.** Spectra of supernatants after conjugation with GNPs and centrifugation. (The background signal of the supernatant without protein G is subtracted.)

The fluorescence values for the supernatants (the fluorescence of nonbound proteins) were compared with the calibration dependence for protein solutions that did not interact with GNPs (fig. 4). The amount of protein bound to GNPs was determined as the difference between total and nonbound amounts.
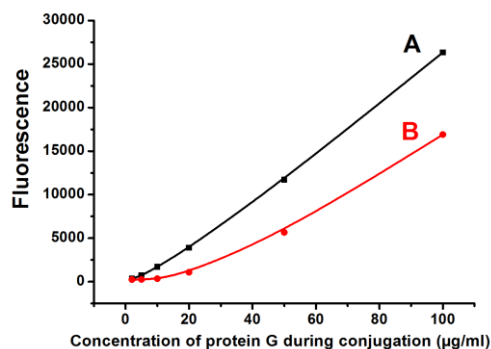

Figure 4. Fluorescence of protein G at an excitation wavelength of 280 nm and an emission wavelength of 350 nm. A. Calibration dependence; B. The supernatant fluorescence after conjugation with GNPs and centrifugation. (Background signal is subtracted.)

The concentration of nanoparticles in experiments to determine the composition of conjugates amounted to 1.59 nM, 3 times higher than in experiments with flocculation. GNPs were concentrated before conjugation to increase the amount of adsorbed protein and reduce the error in determining sorption capacity. Based on the concentration of GNPs, the amount of protein bound to one nanoparticle was calculated (see fig. 5).
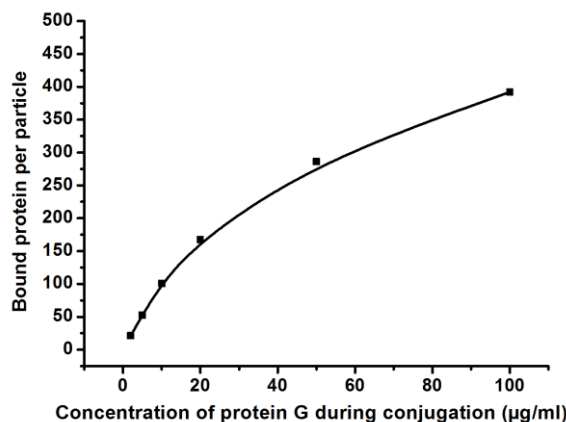

Figure 5. The amount of protein G bound to one GNP, depending on the concentration of the added protein G.

To determine the affinity of protein G binding to the GNP surface, the obtained dependence between the values of free and bound protein was plotted in Sketchard coordinates (as the relationship between the ratio of the amount of bound protein per nanoparticle [X-axis] and the concentration of free protein on the amount of bound protein per nanoparticle [Y-axis]). In these coordinates, the cotangent of the slope of the linearized dependence is equal to the average value of the equilibrium dissociation constant for the complex in a given concentration range; the point of intersection of the linearized dependence with the X-axis gives the maximum number of binding sites for a given dissociation constant. The results are presented in figure 6. The resulting dependence can be divided into three sections with average dissociation constants of 3.4, 11.3, and 212.5 nM.
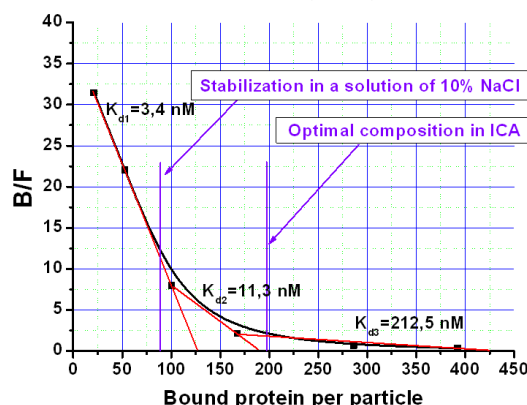

Figure 6. Determination of the equilibrium dissociation constants of the protein G complex with the surface of GNPs in Sketchard coordinates. Red lines indicate linearized sections of the dependence. The violet lines are protein loads that (i) stabilize the conjugates in a solution with high ionic strength and (ii) provide the maximum binding capacity of the conjugate.

The possibility of changing the constants of protein–nanoparticle complexation from units to hundreds of nM was noted in earlier works [22, 29]. An increase in the value of the dissociation constant is easy to explain: when the surface is filled,

the adsorbed protein molecules prevent other molecules from binding to the surface. Figure 6 shows the values of protein corresponding to reaching (i) a plateau of flocculation dependence and (ii) maximum binding capacity of the conjugate. Note that when determining the composition of the conjugates, GNPs were preliminarily concentrated 3 times for more accurate measurements. Therefore, for this nanoparticle preparation, a protein G concentration sufficient to stabilize the conjugates in a solution with high ionic strength was 9 µg/mL. A protein G concentration providing the maximum binding capacity of the conjugate was 24 µg/mL.

The following explanation can be offered for the significant differences between the stabilizing concentration and the concentration that provided the maximum binding ability of the conjugate. Stabilization of nanoparticles occurs when their surface is covered with protein, but the protein molecules are located freely, and the dissociation constant is low (the initial linear portion of the curve in fig. 6). This amount of protein is sufficient to prevent contact of the GNPs with each other and, consequently, to prevent agglutination. However, the surface of the particles is not completely covered. At higher protein concentrations, its adsorption continues, but with lower strength. After binding of 180–200 protein molecules to a particle, the dissociation constant of the complex increases significantly. A further increase in the amount of adsorbed protein does not increase the binding capacity of the conjugate due to partial dissociation of the conjugate and steric factors.

4. CONCLUSIONS

Conjugates of GNPs with streptococcal protein G were tested for composition and antibody-binding capacity. The relationship between these two parameters was established. It was shown that to obtain stable and highly active conjugates, it is necessary to use protein G concentrations corresponding to the point of a sharp increase in the dissociation constant of the conjugate on the Sketchard curve.

5. REFERENCES

1. Cao, Y.; Griffith, B.; Bhomkar, P.; Wishart, D.S.; McDermott, M.T. Functionalized gold nanoparticle-enhanced competitive assay for sensitive small-molecule metabolite detection using surface plasmon resonance. *Analyst* **2018**, *143*, 289-296, https://doi.org/10.1039/C7AN01680H.

2. Singh, P.; Pandit, S.; Mokkapati, V.R.S.S.; Garg, A.; Ravikumar, V.; Mijakovic, I. Gold nanoparticles in diagnostics and therapeutics for human cancer. *International Journal of Molecular Sciences* **2018**, *19*, 1979, https://doi.org/10.3390/ijms19071979.

3. Spicer, C.D.; Jumeaux, C.; Gupta, B.; Stevens, M.M. Peptide and protein nanoparticle conjugates: versatile platforms for biomedical applications. *Chemical Society Reviews* **2018**, *47*, 3574-3620, https://doi.org/10.1039/C7CS00877E.

4. Centi, S.; Ratto, F.; Tatini, F.; Lai, S.; Pini, R. Ready-to-use protein G-conjugated gold nanorods for biosensing and biomedical applications. *Journal of Nanobiotechnology* **2018**, *16*, 5, https://doi.org/10.1186/s12951-017-0329-7.

5. Liu, S.; Haller, E.; Horak, J.; Brandstetter, M.; Heuser, T.; Lämmerhofer, M. Protein A-and Protein G-gold nanoparticle bioconjugates as nano-immunoaffinity platform for human IgG depletion in plasma and antibody extraction from cell culture supernatant. *Talanta* **2019**, *194*, 664-672, https://doi.org/10.1016/j.talanta.2018.10.079.

6. Kang, J.; Yeom, G.; Jang, H.; Oh, J.; Park, C.J., Kim, M.G. Development of replication protein A-conjugated gold nanoparticles for highly sensitive detection of disease biomarkers. *Analytical Chemistry* **2019**, *91*, 10001-10007, https://doi.org/10.1021/acs.analchem.9b01827.

7. Centi, S.; Ratto, F.; Tatini, F.; Lai, S.; Pini, R.. Ready-to-use protein G-conjugated gold nanorods for biosensing and biomedical applications. *Journal of Nanobiotechnology* **2018**, *16*, 5, https://doi.org/10.1186/s12951-017-0329-7.

8. Geoghegan, W.D.; Ackerman, G.A. Adsorption of horseradish peroxidase, ovomucoid and anti-immunoglobulin to colloidal gold for the indirect detection of concanavalin A, wheat germ agglutinin and goat anti-human immunoglobulin G on cell surfaces at the electron microscopic level: a new method, theory and application. *Journal of Histochemistry and Cytochemistry* **1977**, *25*, 1187-1200, https://doi.org/10.1177/25.11.21217.

9. Horisberger, M.; Rosset, J. Colloidal gold, a useful marker for transmission and scanning electron microscopy. *Journal of Histochemistry and Cytochemistry* **1977**, *25*, 295-305, https://doi.org/10.1177/25.4.323352.

10. Pamies, R.; Cifre, J.G.H.; Espín, V.F.; Collado-González, M.; Baños, F.G.D.; de la Torre, J.G. Aggregation behaviour of gold nanoparticles in saline aqueous media. *Journal of Nanoparticle Research* **2014**, *16*, 2376, https://doi.org/10.1007/s11051-014-2376-4.

11. Bell, N.C.; Minelli, C.; Shard, A.G. Quantitation of IgG protein adsorption to gold nanoparticles using particle size measurement. *Analytical Methods* **2013**, *5*, 4591-4601, https://doi.org/10.1039/C3AY40771C.

12. Byzova, N.A.; Safenkova, I.V.; Slutskaya, E.S.; Zherdev, A.V.; Dzantiev, B.B. Less is more: a comparison of antibody–gold nanoparticle conjugates of different ratios. *Bioconjugate Chemistry* **2017**, *28*, 2737-2746, https://doi.org/10.1021/acs.bioconjchem.7b00489.

13. Charbgoo, F.; Nejabat, M.; Abnous, K.; Soltani, F.; Taghdisi, S.M.; Alibolandi, M.; W.T. Shier; T.W.J. Steele; Ramezani, M. Gold nanoparticle should understand protein corona for being a clinical nanomaterial. *Journal of Controlled Release* **2018**, *272*, 39-53. https://doi.org/10.1016/j.jconrel.2018.01.002.

14. Monopoli, M.P.; Walczyk, D.; Campbell, A.; Elia, G.; Lynch, I.; Baldelli, B.F.; Dawson, K.A. Physical− chemical aspects of protein corona: relevance to in vitro and in vivo biological impacts of nanoparticles. *Journal of the American Chemical Society* **2011**, *133*, 2525-2534, https://doi.org/10.1021/ja107583h.

15. Docter, D.; Westmeier, D.; Markiewicz, M.; Stolte, S.; Knauer, S.; Stauber, R. The nanoparticle biomolecule corona: lessons learned–challenge accepted? *Chemical Society Reviews* **2015**, *44*, 6094-6121, https://doi.org/10.1039/c5cs00217f.

16. Pearson, R.M.; Juettner, V.V.; Hong, S. Biomolecular corona on nanoparticles: a survey of recent literature and its implications in targeted drug delivery. *Frontiers in Chemistry* **2014**, *2*, 108, https://doi.org/10.3389/fchem.2014.00108.

17. Liu, W.; Rose, J.; Plantevin, S.; Auffan, M.; Bottero, J.Y.; Vidaud, C. Protein corona formation for nanomaterials and

proteins of a similar size: hard or soft corona? *Nanoscale* **2013,** *5*, 1658-1668, https://doi.org/10.1039/c2nr33611a.

18. Winzen, S.; Schoettler, S.; Baier, G.; Rosenauer, C.; Mailaender, V.; Landfester, K.; Mohr, K. Complementary analysis of the hard and soft protein corona: sample preparation critically effects corona composition. *Nanoscale* **2015,** *7*, 2992-3001, https://doi.org/10.1039/C4NR05982D.

19. Miclaus, T.; Bochenkov, V.E.; Ogaki, R.; Howard, K.A.; Sutherland, D.S. Spatial mapping and quantification of soft and hard protein coronas at silver nanocubes. *Nano Letters* **2014,** *14*, 2086-2093, https://doi.org/10.1021/nl500277c.

20. Waghmare, M.; Khade, B.; Chaudhari, P; Dongre, P. Multiple layer formation of bovine serum albumin on silver nanoparticles revealed by dynamic light scattering and spectroscopic techniques. *Journal of Nanoparticle Research* **2018**, *20*, 185. https://doi.org/10.1007/s11051-018-4286-3.

21. Milani, S.; Baldelli Bombelli, F.; Pitek, A. S.; Dawson, K. A.; Radler, J. Reversible versus irreversible binding of transferrin to polystyrene nanoparticles: soft and hard corona. *ACS Nano* **2012,** *6*, 2532-2541, https://doi.org/10.1021/nn204951s.

22. Sotnikov, D.V.; Zherdev, A.V.; Dzantiev, B.B. Development and application of a label-free fluorescence method for determining the composition of gold nanoparticle–protein conjugates. *International Journal of Molecular Sciences.* **2014,** *16*, 907-923, https://doi.org/10.3390/ijms16010907.

23. Manasa, M.; Revathi, P.; Chand, M.P.; Maroudam, V.; Navaneetha, P.; Raj, G.D.; Kishor, P.K.; De, B.; Rathnagiri, P. Protein-G-based lateral flow assay for rapid serodiagnosis of brucellosis in domesticated animals. *Journal of Immunoassay and Immunochemistry* **2019,** *40*, 149-158, https://doi.org/10.1080/15321819.2018.1541803.

24. Sotnikov, D.V.; Byzova, N.A.; Zherdev, A.V.; Eskendirova, S.Z.; Baltin, K.K.; Mukanov, K.K.; Ramankulov, E.M.; Sadykhov, E.G.; Dzantiev, B.B. Express immunochromatographic detection of antibodies against *Brucella abortus* in cattle sera based on quantitative photometric registration and modulated cut-off level. *Journal of Immunoassay and Immunochemistry* **2015,** *36*, 80-90, https://doi.org/10.1080/15321819.2014.896266.

25. 19. Sun, X.; Zhang, G.; Patel, D.; Stephens, D.; Gobin, A. M. Targeted cancer therapy by immunoconjugated gold–gold sulfide nanoparticles using Protein G as a cofactor. *Annals of Biomedical Engineering* **2012,** *40*, 2131-2139, https://doi.org/10.1007/s10439-012-0575-7.

26. Frens, G. Controlled nucleation for the regulation of the particle size in monodisperse gold suspensions. *Nature physical science* **1973,** *241*, 20, https://doi.org/10.1038/physci241020a0.

27. Byzova, N.A.; Zvereva, E.A.; Zherdev, A.V.; Eremin, S.A.; Sveshnikov, P.G.; Dzantiev, B.B. Pretreatment-free immunochromatographic assay for the detection of streptomycin and its application to the control of milk and dairy products. *Analytica chimica acta* **2011,** *701*, 209-217, https://doi.org/10.1016/j.aca.2011.06.001.

28. Lin, C.T.; Chen, K.J.; Tseng, K.C.; Chu, L.K. Spatially and temporally-resolved tryptophan fluorescence thermometry for monitoring the photothermal processes of gold nanorod suspensions. *Sensors and Actuators B: Chemical* **2018**, *255*, 1285-1290, https://doi.org/10.1016/j.snb.2017.08.112.

29. Ghitescu, L.; Bendayan, M. Immunolabeling efficiency of protein A-gold complexes. *Journal of Histochemistry and Cytochemistry* **1990,** *38*, 1523-1530, https://doi.org/doi:10.1177/38.11.2212613.

6. ACKNOWLEDGEMENTS